MDPI

Arctic Sea Ice Freeboard Retrieval from Envisat Altimetry Data

Shengkai Zhang [ID], Yue Xuan, Jiaxing Li, Tong Geng, Xiao Li and Feng Xiao *[ID]

Chinese Antarctic Center of Surveying and Mapping, Wuhan University, Wuhan 430079, China;
zskai@whu.edu.cn (S.Z.); xuanyue@whu.edu.cn (Y.X.); listening@whu.edu.cn (J.L.); t.geng@whu.edu.cn (T.G.);
lx850569127@whu.edu.cn (X.L.)
* Correspondence: shaw89@whu.edu.cn

Abstract: Arctic sea ice variations are sensitive to Arctic environmental changes and global changes. Freeboard and thickness are two important parameters in sea ice change research. Satellite altimetry can provide long-time and large-scale sea ice monitoring. We estimated the Arctic sea ice freeboard and its variations for the period from 2002 to 2012 from Envisat satellite altimetry data. To remove geoid undulations, we reprocessed the Envisat data using a newly developed mean sea surface (MSS) model, named DTU18. Residuals in the static geoid were removed by using the moving average technique. We then determined the local sea surface height and sea ice freeboard from the Envisat elevation profiles. We validated our freeboard estimates using two radar freeboard products from the European Space Agency (ESA) Climate Change Initiative (CCI) and the Alfred Wegener Institute (AWI), as well as the Operation IceBridge (OIB) sea ice freeboard product. The overall differences between our estimates and the CCI and AWI data were 0.11 ± 0.14 m and 0.12 ± 0.14 m, respectively. Our estimates show good agreement with the three products for areas of freeboard larger than 0.2 m and smaller than 0.3 m. For areas of freeboard larger than 0.3 m, our estimates correlate better with OIB freeboard than with CCI and AWI. The variations in the Arctic sea ice thickness are discussed. The ice freeboard reached its minimum in 2008 during the research period. Sharp decreases were found in the winters of 2005 and 2007.

Keywords: Arctic; sea ice; freeboard; Envisat

1. Introduction

Arctic sea ice has an important role in global climate change [1]. Over the past three decades, the extent and volume of Artic sea ice have decreased continuously [2–4]. Thickness is one of the most important parameters of sea ice [5]. Accurate sea ice thickness retrieval not only benefits Arctic and global change research, but also has significance for polar expeditions and maritime shipping.

Satellite altimetry can provide hemispheric estimates of sea ice thickness. Laxon et al. [6] first estimated the Arctic sea ice thickness using altimetry data from Earth Resource Satellite (ERS-1 and ERS-2) and validated the thickness estimates using draft data from upward-looking sonar. Since then, the altimetric sea ice thickness retrieval method has been widely applied [7–10]. This method first estimates the sea ice freeboard, which is defined as the height of the sea ice surface above the local sea level. The freeboard estimates are then converted to sea ice thickness based on the hydrostatic equilibrium equation.

The uncertainty in freeboard measurements contributes to 40% of the ice thickness uncertainty [8]. The freeboard can be determined from the elevation difference between the sea ice surface and local sea surface. The local sea surface height can be regarded as the lead elevation in sea ice-covered areas. Thus, lead detection is important in sea ice freeboard retrieval. Generally, leads can be detected from waveform parameters such as the pulse peakiness and stack standard deviation for radar altimeters. Lindsay and Rothrock [11] found that leads cover 2% to 3% of the sea ice cover of the Arctic Ocean. Kwok et al. [12] developed a convenient method to derive the lead elevation for retrieving

the Arctic sea ice freeboard. In Kwok's study, leads were considered to be at sea level. The sea surface height at any given point was determined by averaging the lowest 2% of the Ice, Cloud, and land Elevation Satellite (ICESat) elevations within 25 km of that point. Zwally et al. [13] detected leads in at least 2% of a 50 km section of an ICESat elevation profile and subsequently determined the local sea level by averaging the lowest 2% of the relative elevations. Skorup et al. [14] determined the sea level by averaging the three lowest elevations in a 20 km section of an ICESat profile.

Tilling et al. [15] found that the uncertainty in sea surface determination is the main contributor to thickness uncertainty in first-year ice thickness retrieval. Due to the limited accuracy of the geoid and ocean tide models, sea ice surface elevations are usually referenced to the mean sea surface (MSS) in freeboard retrieval. Peacock et al. [7] used the Earth Gravitational Model 1996 (EGM96) to compute the long-wavelength components of the geoid in extracting sea surface height from ERS-1/2 data. Schwegmann et al. [16] used the Danish Technical University 2015 (DTU15) MSS model [17] to remove the effect of geoid undulations while estimating the South Ocean sea ice freeboard using Envisat and CryoSat-2 data. Skourup et al. [18] evaluated the implications for sea ice freeboard retrieval with different MSS models and the geoid models. The results showed that sea ice freeboard retrievals from airborne/satellite altimeter measurements are impacted by the choice of MSS or geoid model used in the retrieval algorithm. The impact of remaining MSS/GGM errors on freeboard retrieval can reach several decimeters in parts of the Arctic.

In this study, we derived the Arctic sea ice freeboard from Envisat altimetry data by applying Kwok's method. A newly developed MSS model, namely, the DTU18, was used to remove the geoid undulations. The freeboard results were compared with two radar freeboard products and the Operation IceBridge (OIB) freeboard.

2. Data

2.1. Envisat Data

Envisat was launched in March 2002 by the European Space Agency (ESA) and was once the largest Earth observation spacecraft, providing coverage of the Arctic Ocean up to 81.5° N. The Envisat mission was ended in April 2012 and it delivered thousands of images and a wealth of data used to study the workings of the Earth's systems. Envisat had 10 instruments, including the Radar Altimeter-2 (RA-2), to provide continuous observation and monitoring of the Earth. The RA-2 altimeter is a dual-frequency, nadir-pointing, pulse-limited radar operating at 13.575 GHz (Ku-band) and 3.2 GHz (S-band) using a single antenna dish. It is designed to operate autonomously and without interruption over all surfaces: ocean, land, and ice.

ESA provides processed Envisat data as a Level 2 product, including the Geophysical Data Record (GDR), Sensor Geophysical Data Record and Marine Abridged Records. The GDR product published in 2011 (version 2.1) was used in this study to retrieve the Arctic sea ice freeboard. The GDR product contains datation, geolocation, output from retrackers, and surface type flags. The product also includes additional information, such as geophysical and tidal corrections and quality flags [19].

2.2. Mean Sea Surface Models

The MSS model plays an important role in sea ice freeboard calculation [18]. Table 1 presents a comparison of typical MSS models. The Envisat L2 product provides the MSS height from the Collecte Localisation Satellites 2001 (CLS01) model [20]. The Technical University of Denmark (DTU) have published a series of MSS models based on satellite altimetry data. The newest MSS model from DTU is DTU18 [21], which provides the global MSS height at a resolution of $1' \times 1'$. The DTU18 model utilizes satellite altimetry data, including Topex/Poseidon (T/P), Jason 1/2, ERS-1/2, Envisat, CryoSat-2, SARAL/Altika, and Sentinel-3A. DTU18 contains significant improvements in terms of satellite altimetry time series and resolution compared to CLS01.

Table 1. A comparison of three widely used mean sea surface (MSS) models.

	CLS01	DTU15	DTU18
Reference ellipsoid	T/P	T/P	T/P
Time period	1993–1999	1991–2015	1993–2017
coverage	80° S–82° N	90° S–90° N	90° S–90° N
Grid resolution	2′ × 2′	1′ × 1′	1′ × 1′
Data sources	ERS-1/2, GEOSAT and T/P	T/P, Jason 1/2, ERS-1/2, Envisat and CryoSat-2	T/P, Jason 1/2, ERS-1/2, Envisat, CryoSat-2, SARAL/Altika and Sentinel-3A

2.3. Sea Ice Freeboard Products

To validate the accuracy of our sea ice freeboard estimates, we employed sea ice freeboard products from the ESA Climate Change Initiative (CCI) [22], the Alfred Wegener Institute (AWI) [23], and the National Snow and Ice Data Center (NSIDC) [24].

The CCI product provides monthly Arctic sea ice thickness and freeboard data on a 25 km grid for the period of October 2002 to March 2012, from the RA-2 instrument on the Envisat satellite. AWI provides a monthly Arctic sea ice freeboard product on a 25 km grid from CryoSat-2 altimetry data for the period from November 2010 to the present. The CCI and AWI products are only available for the winter months of October through April. The DTU15 MSL model was used by CCI and AWI to retrieve the sea ice freeboard.

The sea ice freeboard from NSIDC is based on airborne measurements from Operation IceBridge (OIB). OIB measures the sea ice freeboard and snow depth using an onboard airborne topographic mapper and snow radar. The OIB product is available at a 40 m spatial sampling resolution along the flight lines. More than 50,000 OIB measurements from the period of March 16 to 23 and March 25 to 28 in 2011 were used for validation.

3. Methodology

Figure 1 provides an outline of the steps in our data processing chain. We used geolocated elevations from the ESA Envisat GDR product. Before estimating the freeboard, geophysical corrections, including inverse barometer, sea state bias, ionospheric correction, dry/wet tropospheric correction, and tide correction, were applied to the elevation points. These geophysical corrections can be obtained from the GDR product. Table 2 shows the models and data sources used for geophysical corrections in the GDR data.

Table 2. Models and data sources used for geophysical corrections in Geophysical Data Record (GDR) data.

Geophysical Corrections	Models or Sources☐
Inverse Barometer	ECMWF
Sea State Bias	Envisat Ku-band's significant wave height and the RA-2 wind speed
Ionospheric Correction	the DORIS daily TEC maps
Ocean Tide	GOT00.2b
Polar Tide	IERS Centre
Wet Tropospheric Correction	ECMWF
Dry Tropospheric Correction	ECMWF

The sea ice freeboard can be determined from the elevation difference between the sea ice surface and local sea surface:

$$h_f = h - h_{ssh} \tag{1}$$

where h_f is the sea ice freeboard, h is the ellipsoidal height of the sea ice surface from Envisat, and h_{ssh} is the local sea surface height.

Firstly, geoid undulations are removed by subtracting the MSS height (h_{mss}) [19]:
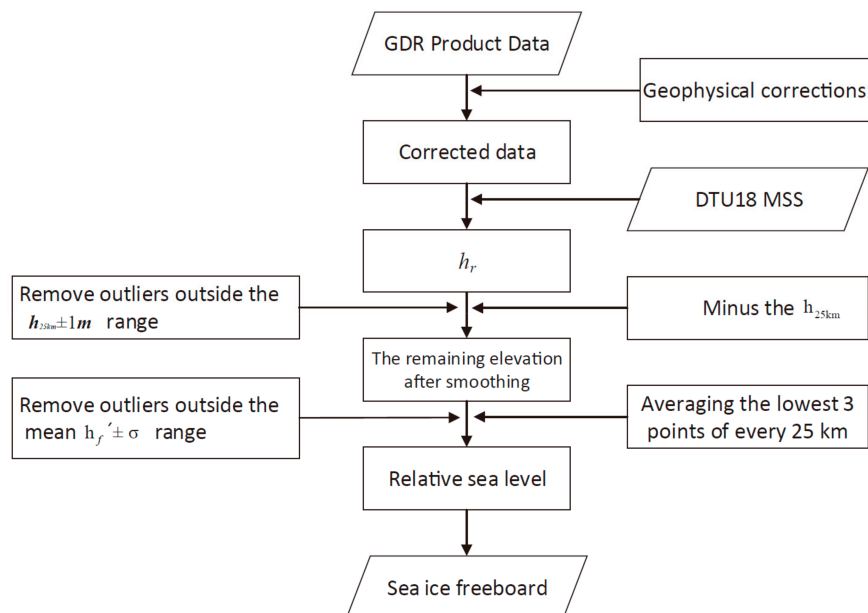
$$h_r = h - h_{mss}. \tag{2}$$

Figure 1. A flowchart of the freeboard retrieval algorithm.

Here, h_r denotes the relative elevation. Figure 2 shows a comparison of relative elevation profiles with reference to CLS01, DTU15 and DTU18. The relative elevations with CLS01 still contains residuals of the geoid undulations in areas with large mean sea surface fluctuation due to the poor spatial resolution, while the relative elevations with DTU15 and DTU18 are much smoother, which means the two MSS models perform better in removing geoid undulations. The relative elevations from DTU15 and DTU18 show minor differences. However, DTU18 includes more satellite altimetry observations (SARAL/Altika, Sentinel-3A and longer CryoSat-2 observation time series) than DTU15. So, we employed the DTU18 model in the calculation.

Kwok et al. [12] found that the residuals in sea surface height are much greater than the expected magnitude of sea ice freeboard, and consequently, they used a 25 km running mean of h_r to remove the residuals. We followed Kwok's method to obtain the modified relative elevations:

$$h_r' = h_r - h_{25km} \tag{3}$$

where h_{25km} is the 25 km running mean of h_r. Figure 3 shows a sample of the Envisat elevation profiles of h_r and h_r'. To ensure the integrity of valid data and to eliminate exceptional values, we first calculated the standard deviation (SD) of h_r' in every 25 km section of the Envisat profile. Elevations beyond $h_{25km} \pm n \cdot SD$ were regarded as outliers according to the error processing criterion. n refers to multiples of the SD. As shown in Figure 4 and Table 3, we tested different multiples of the SD to filter the data. Figure 4 shows the elimination results of different multiples of the standard deviation, and Table 2 presents the statistics for the different rejection methods. Outliers still remained for $n = 3$ and $n = 2$. However, when $n = 0.5$, a large number of data, including some useful information, were eliminated. From Figure 4c, we can see that the distribution of the relative elevation was at a sensible level and the integrity of the data was guaranteed with $n = 1$.
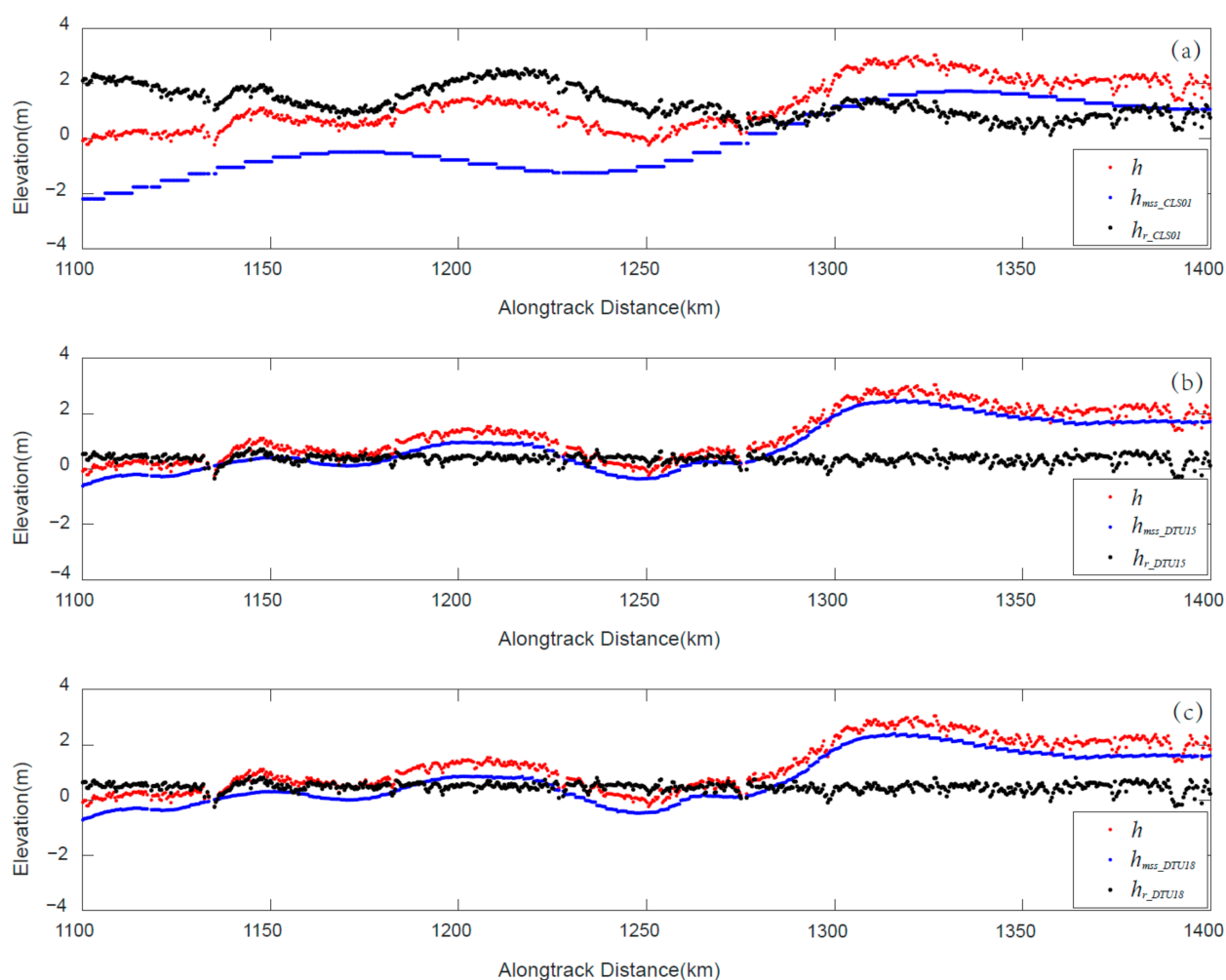
Figure 2. A sample of Envisat elevation profiles over the Arctic Ocean. The red points in (**a**–**c**) represent the reference elevation to the WGS84 ellipsoid. The blue points in (**a**–**c**) represent the mean sea surface height from CLS01, DTU15 and DTU18, respectively. The black points in (**a**–**c**) represent the relative elevations with CLS01, DTU15 and DTU18, respectively.
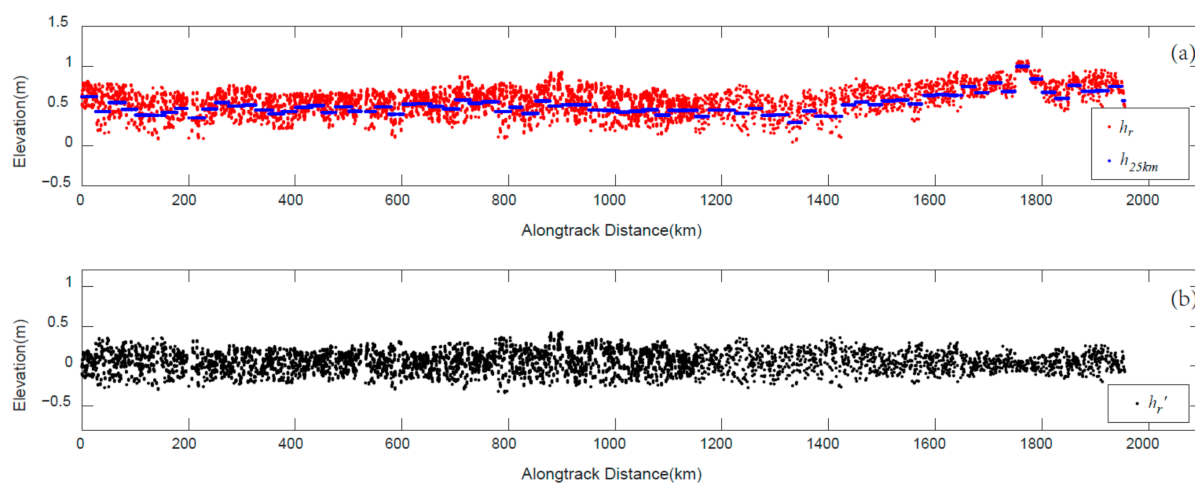

Figure 3. A sample of Envisat elevation profiles. The red points in (**a**) are the relative elevation h_r values; the blue points in (**a**) are h_{25km} values, defined as the 25 km running mean of h_r; and the black points in (**b**) are the modified relative elevation h_r' values.
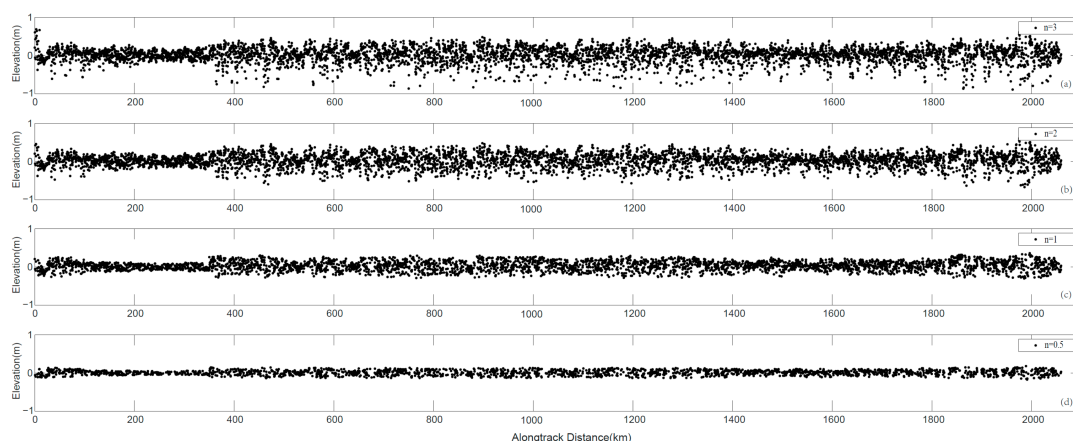
Figure 4. Outlier elimination results for different multiples of the standard deviation: (**a**) *n* = 3, (**b**) *n* = 2, (**c**) *n* = 1, (**d**) *n* = 0.5.

Table 3. Rejection rates for different multiples of the standard deviation.

Orbit	Number of the Original Points	*n* = 3		*n* = 2		*n* = 1		*n* = 0.5	
		Number of Points after Elimination	Rejection Rate (%)	Number of Points after Elimination	Rejection Rate (%)	Number of Points after Elimination	Rejection Rate (%)	Number of Points after Elimination	Rejection Rate (%)
19654	5492	5269	1.40	5083	4.88	3934	26.38	2239	58.10
19726	5655	5447	1.48	5238	5.26	4121	25.47	2309	58.24
19780	10302	9738	1.10	9328	5.26	7187	27.01	3950	59.88
19883	5451	5226	1.12	5045	4.54	3795	28.19	2115	59.98
19926	5602	5366	1.41	5160	5.20	3999	26.53	2212	59.36

Next, we can determine the local sea surface height from the modified relative elevation profiles. Leads in sea ice are considered to be at sea level. We determined our sea level (h_{ssh}) by averaging the three lowest elevations in a 25 km section of an Envisat profile. Finally, the sea ice freeboard can be determined by

$$h_f = h'_r - h_{ssh}. \tag{4}$$

Figure 5 shows an example of sea ice freeboard estimation results from an Envisat elevation profile. The mean freeboard of this profile is 0.162 m, the majority of the freeboard is within the range of 0 to 0.3 m.
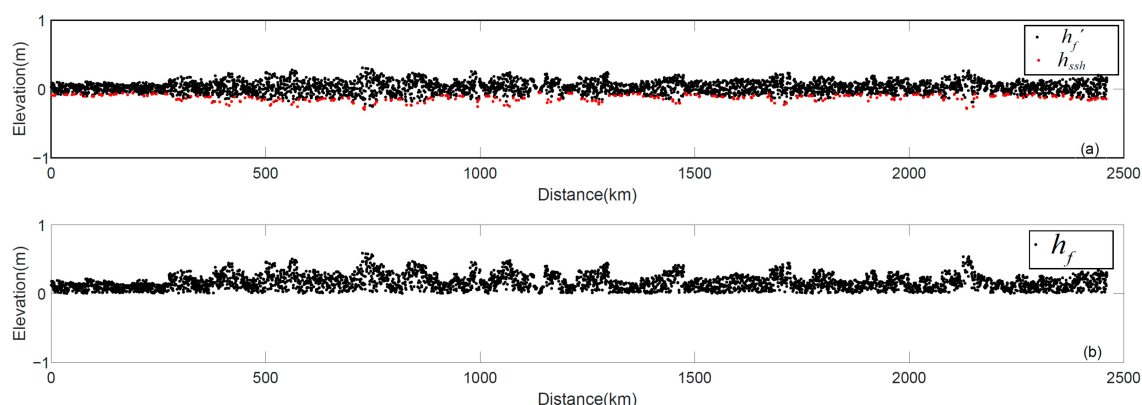

Figure 5. A sample of sea ice freeboard estimation results from an Envisat profile. The black points in (**a**) indicate the modified relative elevation (h'_r), the red points in (**a**) indicate the sea level (h_{ssh}), and the black points in (**b**) indicate the retrieved sea ice freeboard (h_f).

4. Arctic Sea Ice Freeboard Estimation Results and Validation

4.1. Arctic Sea Ice Freeboard Estimation Results

We derived the Arctic sea ice freeboard for October 2002 through April 2012 from Envisat data. We did not estimate the sea ice freeboard for the months of May to September due to the existence of melt ponds. Figure 6 shows an example of the spatial distribution of the sea ice freeboard for the sea ice growth season of 2009/2010. Figure 7 shows the mean sea ice freeboard of the Arctic freeboard during the growth season. In October, the sea ice freeboard was the smallest with an average value of 0.167 m. The sea ice distribution in October was concentrated in the Beaufort Sea and north of the Canadian Arctic Archipelago. In November, the sea ice extent increased and sea ice began to appear in the East Siberian and Barents Seas. The average sea freeboard in November was 0.179 m. In December and January, the sea ice freeboard continued to grow and reached 0.195 m in January. In February, the freeboard growth rate showed a slight decline with an average freeboard of 0.199 m. In March and April, the thick sea ice extent increased, especially in the Chukchi Sea and Canadian Arctic Archipelago. The sea ice freeboard reached a maximum of 0.223 m in April. During the 2009/2010 sea ice growth season, the freeboard growth rate of the Arctic Ocean was 0.008 m per month.
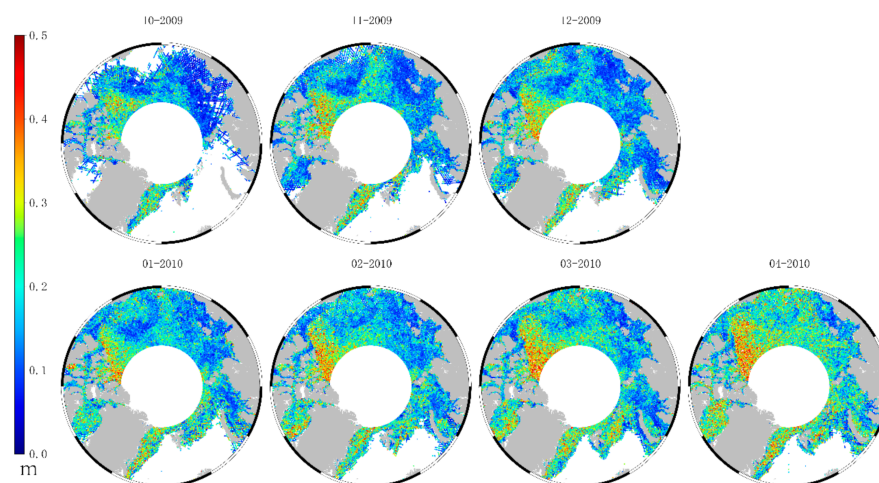

Figure 6. The sea ice freeboard distribution for the 2009/2010 Arctic sea ice growth season from October to April.
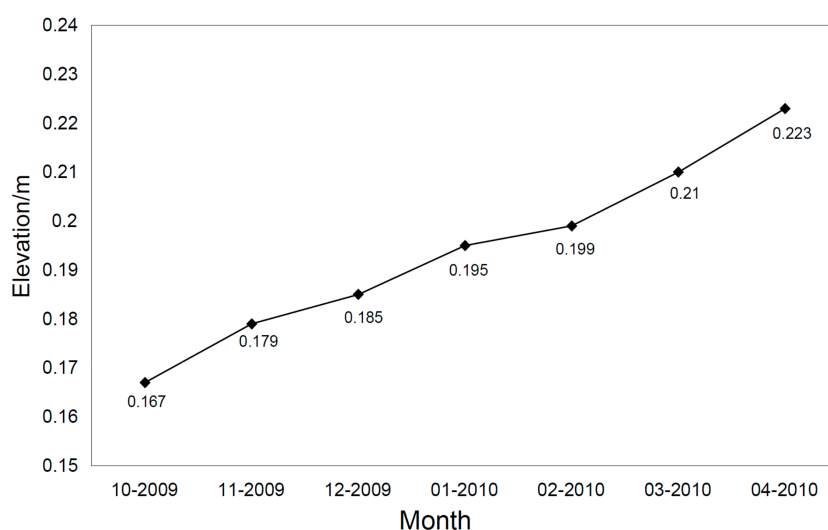

Figure 7. Mean sea ice freeboard variations in the Arctic Ocean for the 2009/2010 Arctic sea ice growth season from October to April.

4.2. Comparison with Sea Ice Freeboard Products

Comparisons between our sea ice freeboard retrieval and two satellite sea ice freeboard products (AWI and CCI) were performed. The comparisons with the CCI sea ice freeboard were conducted for the period of October 2010 to April 2011, and for AWI, the period was from November 2010 to April 2011. Our Envisat freeboard estimates were allocated into the 25 km resolution grid. The averaged Envisat freeboard in a certain grid cell was compared with those from CCI and AWI. Table 4 shows the mean values, root-mean-squared errors (RMSE) and standard deviations (STD) of the comparisons. The overall differences between our estimates and CCI and AWI data were 0.11 ± 0.09 m and 0.12 ± 0.08 m, respectively. The RMSE of the bias between our estimates and the two products are very close for each month; they varied from 0.13 to 0.15 m. The differences between our freeboard estimates and the two products are small. The bias was a little larger at the beginning of the sea ice growth season.

Table 4. Bias between the sea ice freeboards retrieved in this study and that from CCI and AWI.

Month	This Study–CCI			This Study–AWI		
	Bias/m	RMSE/m	STD/m	Bias/m	RMSE/m	STD/m
October 2010	0.12	0.15	0.09			
November 2010	0.12	0.14	0.08	0.13	0.15	0.07
December 2010	0.11	0.14	0.08	0.13	0.14	0.07
January 2011	0.11	0.13	0.08	0.12	0.14	0.07
February 2011	0.09	0.13	0.09	0.11	0.13	0.08
March 2011	0.1	0.13	0.09	0.11	0.13	0.09
April 2011	0.09	0.14	0.10	0.11	0.14	0.09
Overall	0.11	0.14	0.09	0.12	0.14	0.08

To illustrate how our estimates performed in different freeboard ranges, we allocated the bias between our estimates and the two products into seven freeboard ranges. Figure 8 shows the histograms of the freeboard bias between this study and the two products. The two biases have near normal distributions. Tables 5 and 6 show the statistics of the bias in these different freeboard ranges for our estimates versus CCI and AWI data, respectively. The majority of the bias was distributed in thin-ice-covered areas (freeboard smaller than 0.1 m). Our estimates showed a 0.12 m and 0.13 m bias against the two products in thin-ice-covered areas. The difference was smallest in areas of freeboard larger than 0.2 m and smaller than 0.3 m. The bias increased with freeboard height in areas of freeboard larger than 0.3 m. However, less than 2% of the bias was distributed in these areas.
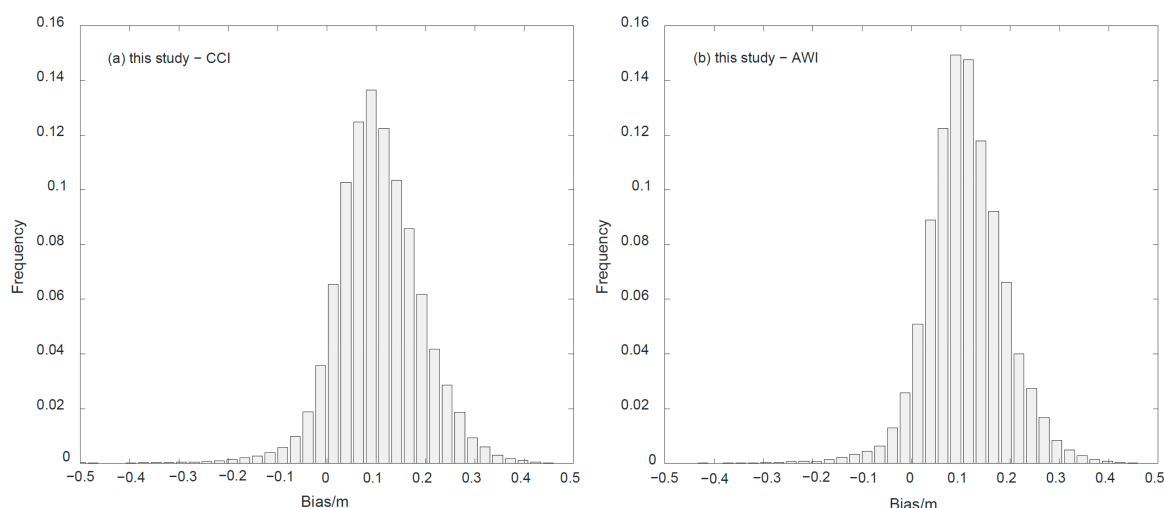

Figure 8. Histograms of the freeboard bias between this study and the two products, (**a**) this study and CCI, (**b**) this study and AWI.

Table 5. Bias between the freeboard from this study and that from CCI in different freeboard ranges.

Freeboard Range/m	Bias/m	RMSE/m	Number of Points
0—0.1	0.12	0.14	32,767
0.1—0.2	0.07	0.10	16,654
0.2—0.3	0.00	0.08	2055
0.3—0.4	−0.10	0.13	550
0.4—0.5	−0.21	0.23	213
0.5—0.6	−0.34	0.35	58
0.6—0.7	−0.45	0.46	26

Table 6. Bias between the freeboard from this study and that from AWI in different freeboard ranges.

Freeboard Range/m	Bias/m	RMSE/m	Number of Points
0–0.1	0.13	0.14	32,542
0.1–0.2	0.09	0.11	12,604
0.2–0.3	0.02	0.08	1980
0.3–0.4	−0.08	0.11	612
0.4–0.5	−0.17	0.19	181
0.5–0.6	−0.32	0.34	40
0.6–0.7	−0.44	0.44	9

4.3. Validation Using the IceBridge Freeboard

To further assess our sea ice freeboard estimates, we compared our results, as well as the freeboard data from CCI and AWI, with the OIB sea ice freeboard. As shown in Figure 9d, the ice freeboard results from the tracks within the Envisat period were used for comparison. The freeboard from Envisat and CryoSat-2 (radar freeboard) is defined as the height of sea ice above the ocean, while the freeboard from OIB (laser freeboard) is the height of snow cover and sea ice above the ocean. So, before the comparison, the laser freeboard was corrected to the radar freeboard by using snow depth from the OIB snow radar. The modified OIB freeboard were then allocated into a 25 km resolution grid. The averaged OIB freeboard in a certain grid cell was compared with radar freeboards.

Figure 9 shows scatterplots of the sea ice freeboard estimated in this study and that from the two products against that from OIB. Table 7 presents statistics relating to the comparison. Our results showed the best performance versus OIB with a mean bias of 0.01 m and RMSE of 0.06 m. The difference between CCI and OIB was about −0.05 ± 0.09 m, and −0.07 ± 0.07 m for AWI versus OIB. The correlations between the three radar freeboards and OIB freeboard vary from 0.65 and 0.79. We can see from Figure 9 that the majority of the sea ice freeboard estimates from AWI and CCI are smaller than those from OIB, while our estimates are a bit larger than the OIB freeboard. Recent research demonstrates that radar signals may only partially penetrate into the snow layer [23]. So, the radar freeboard is the sum of the ice freeboard and unpenetrated snow depth, and the radar freeboard will be larger than the modified OIB freeboard.

Table 7. Statistics of the comparison of the sea ice freeboard across this study, the two products, and OIB.

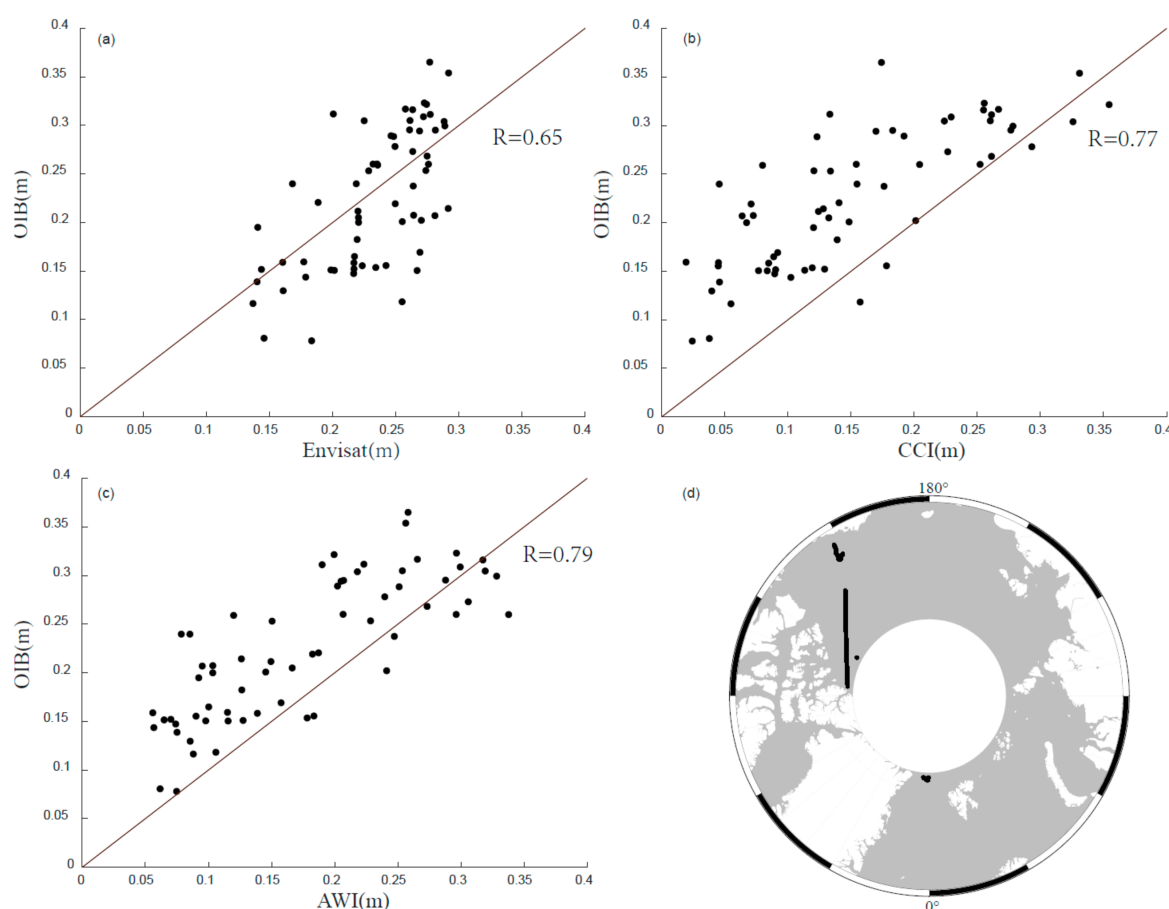|	Mean Bias/m	RMSE/m	Correlation Coefficient
This study vs. OIB	0.01	0.06	0.65
CCI vs. OIB	−0.05	0.09	0.77
AWI vs. OIB	−0.07	0.07	0.79

Figure 9. Scatterplots of the sea ice freeboard from this study and that from the two products versus that from Operation IceBridge (OIB): (**a**) this study vs. OIB, (**b**) CCI vs. OIB, (**c**) AWI vs. OIB. (**d**) illustrates the OIB tracks (black lines) within the Envisat mission period.

5. Discussion

The validation results demonstrate that our freeboard estimates have equal accuracy with the two freeboard products from CCI and AWI. The main difference between this study and previous studies of freeboard retrieval with radar altimeter data is the leads detection method. Leads are usually detected with radar waveform parameters, which requires complex waveform retracking and a large amount of calculation. In this study, we first optimized the elevation profile from Envisat by applying the high accuracy MSS model and an appropriate outlier elimination method. Then, we detected leads and local sea level from the elevation profiles. Our method features less computation and close accuracy with other products.

Satellite observations demonstrate that the Arctic sea ice freeboard and thickness has decreased continuously over the past several decades. We derived the annual and monthly variations in the Arctic sea ice freeboard based on our freeboard estimates. Figure 10 shows the annual average sea ice freeboard variations from 2003 to 2011. As there were only three months' observations and four months' observations for 2002 and 2012, respectively, the annual average freeboard variations for these two years were not considered. Overall, the sea ice freeboard followed a decreasing trend from 2003 to 2011. From 2003 to 2008, the annual average ice freeboard decreased at a rate of 0.005 m per year. In 2008, the ice freeboard reached a minimum of 0.188 m during the research period. In 2009, the ice freeboard increased slightly (0.001 m), while in 2010, the freeboard increased sharply (0.008 m) and reached 0.197 m. In 2011, the sea ice freeboard showed a large decrease of 0.008 m.
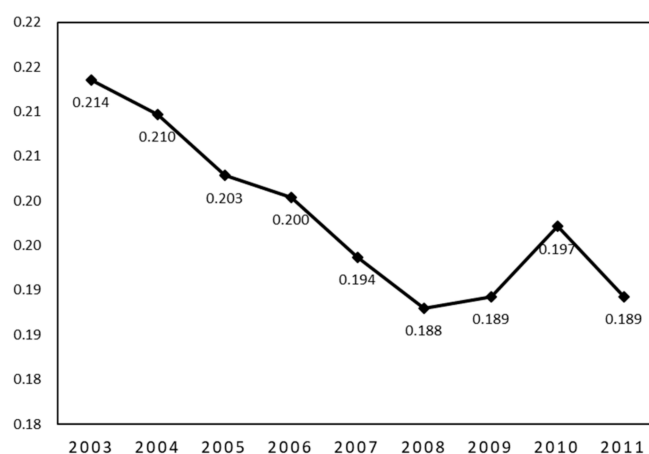
Figure 10. Annual average sea ice freeboard variations in the Arctic Ocean from 2003 to 2011.

Figure 11 shows the monthly average freeboard variations in the Arctic sea ice from October 2002 to April 2012. Seasonal variations can be clearly found in the Arctic sea ice freeboard. The sea ice freeboard increased each month over a certain sea ice growth season from October until April but this was punctuated with some variability from month to month. For example, in some years (e.g., 2004, 2006, 2008, 2011), the ice freeboard decreased in November or December. This is mainly because there was more thin ice in November and December, which reduced the overall sea ice thickness.
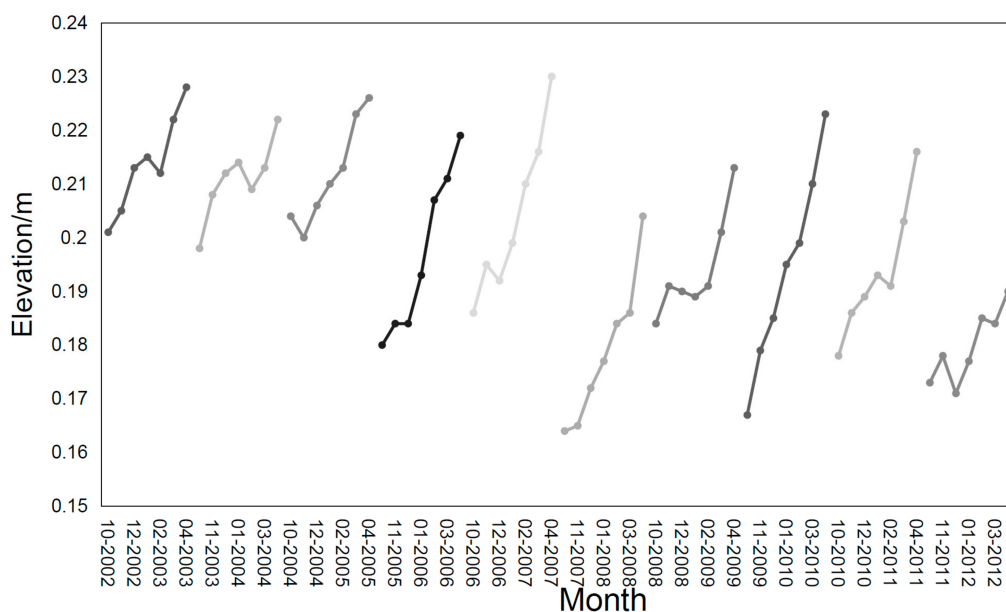

Figure 11. Monthly average sea ice freeboard variations in the Arctic Ocean from October 2002 to April 2012.

The monthly average freeboard reached a minimum in October 2007. This notable decrease in sea ice freeboard has also been reported by other researchers. Giles et al. [25] attributed the reduction to greater exposure of the ocean during the summer. This undue exposure inhibited ice growth in the following winter. Kwok et al. [26–28] showed that after the record minimum in summer extended through 2007, the sea ice thickness showed near zero replenishment until the end of 2013.

6. Conclusions

In this study, we have presented a convenient and fast process for freeboard retrieval with radar altimetry. Our method features less computation and has close accuracy with

other products. First, we evaluated the implications of three widely used MSS models in removing the residuals of the geoid undulations. The DTU18 MSS model performed best and was used for the calculation. We then optimized the elevation profile from Envisat by applying the high accuracy DTU18 MSS model and an appropriate outlier elimination method. Finally, we derived the local sea level and sea ice freeboard from the modified Envisat elevation profiles.

To validate our results, the freeboard estimates were compared with freeboard results from CCI and AWI. The overall difference between the freeboard in this study and that from CCI was 0.11 ± 0.14 m, and the difference was 0.12 ± 0.14 m compared with AWI. The main difference between our freeboard estimates and those from the two products was found in thin-ice-covered areas. We also validated our estimates using OIB freeboard data. Our results showed good agreement with OIB data, with a difference of 0.01 ± 0.06 m.

We were able to derive the Arctic sea ice freeboard estimates from 2002 to 2012 with our method. Annual and monthly variations of the Arctic sea ice freeboard were analyzed. The Arctic sea ice freeboard decreased from 2002 to 2012. The ice freeboard reached its minimum in 2008 during the research period. From the monthly sea ice freeboard variations, we found two obvious reductions in the winters of 2007 and 2009. This is due to the over exposure of the ocean during the summer. The ice freeboard showed rebounds in growth after these two sharp decreases.

Author Contributions: S.Z. and Y.X. conceived and performed the experiments, wrote the main manuscript; F.X. provided critical comments and contributed to the final revision of the paper; J.L., T.G. and X.L. helped with the writing of the data. All authors have read and agreed to the published version of the manuscript.

Institutional Review Board Statement: Not applicable for studies not involving humans or animals.

Informed Consent Statement: Not applicable for studies not involving humans.

Data Availability Statement: The data that support the findings of this study are available from the author upon reasonable request.

Conflicts of Interest: The authors declare no conflict of interest.

References

1. Holland, M.M.; Bitz, C.M. Polar amplification of climate change in coupled models. *Clim. Dyn.* **2003**, *21*, 221–232. [CrossRef]
2. Rothrock, D.A.; Yu, Y.; Maykut, G.A. Thinning of the Arctic sea-ice cover. *Geophys. Res. Lett.* **1999**, *26*, 3469–3472. [CrossRef]
3. Rothrock, D.A.; Percival, D.B.; Wensnahan, M. The decline in arctic sea-ice thickness: Separating the spatial, annual, and interannual variability in a quarter century of submarine data. *J. Geophys. Res. Ocean.* **2008**, *113*. [CrossRef]
4. Lindsay, R.; Schweiger, A. Arctic sea ice thickness loss determined using subsurface, aircraft, and satellite observations. *Cryosphere* **2015**, *9*, 269–283. [CrossRef]
5. Zwally, H.J.; Comiso, J.C.; Parkinson, C.L.; Cavalieri, D.J.; Gloersen, P. Variability of Antarctic sea ice 1979–1998. *J. Geophys. Res. Ocean.* **2002**, *107*, 9-1–9-19. [CrossRef]
6. Laxon, S.; Peacock, N.; Smith, D. High interannual variability of sea ice thickness in the Arctic region. *Nature* **2003**, *425*, 947–950. [CrossRef] [PubMed]
7. Peacock, N.R.; Laxon, S.W. Sea surface height determination in the Arctic Ocean from ERS altimetry. *J. Geophys. Res. Ocean.* **2004**, *109*. [CrossRef]
8. Alexandrov, V.; Sandven, S.; Wahlin, J.; Johannessen, O.M. The relation between sea ice thickness and freeboard in the Arctic. *Cryosphere* **2010**, *4*, 373–380. [CrossRef]
9. Connor, L.N.; Laxon, S.W.; Ridout, A.L.; Krabill, W.B.; McAdoo, D.C. Comparison of Envisat radar and airborne laser altimeter measurements over Arctic sea ice. *Remote Sens. Environ.* **2009**, *113*, 563–570. [CrossRef]

10. Xiao, F.; Li, F.; Zhang, S.; Li, J.; Geng, T.; Xuan, Y. Estimating Arctic Sea Ice Thickness with CryoSat-2 Altimetry Data Using the Least Squares Adjustment Method. *Sensors* **2020**, *20*, 7011. [CrossRef]

11. Lindsay, R.W.; Rothrock, D.A. Arctic sea ice leads from advanced very high resolution radiometer images. *J. Geophys. Res. Ocean.* **1995**, *100*, 4533–4544. [CrossRef]

12. Kwok, R.; Cunningham, G.F.; Zwally, H.J.; Yi, D. Ice, Cloud, and land Elevation Satellite (ICESat) over Arctic sea ice: Retrieval of freeboard. *J. Geophys. Res. Ocean.* **2007**, *112*. [CrossRef]

13. Zwally, H.J.; Yi, D.; Kwok, R.; Zhao, Y. ICESat measurements of sea ice freeboard and estimates of sea ice thickness in the Weddell Sea. *J. Geophys. Res. Ocean.* **2008**, *113*. [CrossRef]

14. Skourup, H.; Forsberg, R. Sea ice freeboards from ICESat—A comparison to airborne lidar measurements. In *Arctic Sea Ice Thickness: Past, Present and Future*; Springer: Berlin/Heidelberg, Germany, 2006; pp. 82–92.

15. Tilling, R.; Ridout, A.; Shepherd, A. Assessing the impact of lead and floe sampling on Arctic sea ice thickness estimates from Envisat and CryoSat-2. *J. Geophys. Res. Ocean.* **2019**, *124*, 7473–7485. [CrossRef]

16. Schwegmann, S.; Rinne, E.; Ricker, R.; Hendricks, S.; Helm, V. About the consistency between Envisat and CryoSat-2 radar freeboard retrieval over Antarctic sea ice. *Cryosphere* **2016**, *10*, 1415–1425. [CrossRef]

17. Andersen, O.B.; Stenseng, L.; Piccioni, G.; Knudsen, P. The DTU15 MSS (mean sea surface) and DTU15 LAT (lowest astronomical tide) reference surface. In Proceedings of the ESA Living Planet Symposium, Prague, Czech Republic, 9–13 May 2016; Available online: https://ftp.space.dtu.dk/pub/DTU15/DOCMENTS/MSS/DTU15MSS\T1\thLAT.pdf (accessed on 12 October 2020).

18. Skourup, H.; Farrell, S.L.; Hendricks, S.; Ricker, R.; Armitage, T.W.; Ridout, A.; Baker, S. An assessment of state-of-the-art mean sea surface and geoid models of the Arctic Ocean: Implications for sea ice freeboard retrieval. *J. Geophys. Res. Ocean.* **2017**, *122*, 8593–8613. [CrossRef]

19. Ollivier, A.; Faugere, Y.; Picot, N.; Ablain, M.; Femenias, P.; Benveniste, J. Envisat ocean altimeter becoming relevant for mean sea level trend studies. *Mar. Geod.* **2012**, *35*, 118–136. [CrossRef]

20. Hernandez, F.; Schaeffer, P. *The CLS01 Mean Sea Surface: A validation with the GSFC00. 1 Surface*; CLS Ramonville St Agne: Ramonville-Saint-Agne, France, 2001.

21. Andersen, O.; Knudsen, P.; Stenseng, L. A new DTU18 MSS mean sea surface–Improvement from SAR altimetry. In Proceedings of the 25 Years of Progress in Radar Altimetry Symposium, Azores Archipelago, Portugal, 24–29 September 2018.

22. Hendricks, S.; Paul, S.; Rinne, E. ESA Sea Ice Climate Change Initiative (Sea_Ice_cci). Northern hemisphere sea ice thickness from the Envisat satellite on a monthly grid (L3C), v2.0. *Cent. Environ. Data Anal.* **2018**. [CrossRef]

23. Ricker, R.; Hendricks, S.; Helm, V.; Skourup, H.; Davidson, M. Sensitivity of CryoSat-2 Arctic sea-ice freeboard and thickness on radar-waveform interpretation. *Cryosphere* **2014**, *8*, 1607–1622. [CrossRef]

24. Kurtz, N.T.; Farrell, S.L.; Studinger, M.; Galin, N.; Harbeck, J.P.; Lindsay, R.; Onana, V.D.; Panzer, B.; Sonntag, J.G. Sea ice thickness, freeboard, and snow depth products from Operation IceBridge airborne data. *Cryosphere* **2013**, *7*, 1035–1056. [CrossRef]

25. Giles, K.A.; Laxon, S.W.; Ridout, A.L. Circumpolar thinning of Arctic sea ice following the 2007 record ice extent 311 minimum. *Geophys. Res. Lett.* **2008**, *35*. [CrossRef]

26. Kwok, R.; Cunningham, G.F. Deformation of the Arctic Ocean ice cover after the 2007 record minimum in summer ice extent. *Cold Reg. Sci. Technol.* **2012**, *76*, 17–23. [CrossRef]

27. Kwok, R.; Cunningham, G.F.; Wensnahan, M.; Rigor, I.; Zwally, H.J.; Yi, D. Thinning and volume loss of the Arctic Ocean sea ice cover: 2003–2008. *J. Geophys. Res. Ocean.* **2009**, *114*. [CrossRef]

28. Kwok, R.; Cunningham, G.F. Variability of Arctic sea ice thickness and volume from CryoSat-2. *Philos. Trans. R. Soc. A Math. Phys. Eng. Sci.* **2015**, *373*, 20140157. [CrossRef] [PubMed]